J|A|C|S ARTICLES

Published on Web 05/04/2009

Inhibition of Human Sirtuins by in Situ Generation of an Acetylated Lysine−ADP−Ribose Conjugate

Tomomi Asaba, Takayoshi Suzuki,* Rie Ueda, Hiroki Tsumoto, Hidehiko Nakagawa, and Naoki Miyata*

Graduate School of Pharmaceutical Sciences, Nagoya City University, 3-1 Tanabe-dori, Mizuho-ku, Nagoya, Aichi 467-8603, Japan

Received September 7, 2008; E-mail: suzuki@phar.nagoya-cu.ac.jp; miyata-n@phar.nagoya-cu.ac.jp

Abstract: A new type of small-molecular sirtuin inhibitor was designed on the basis of the proposed catalytic mechanism for deacetylation of acetylated lysine substrates by sirtuins. Among the compounds thus designed and synthesized, we found that **2k**, which contains an ethoxycarbonyl group at the α position to the acetamide of acetylated lysine substrate analogue **1**, showed potent inhibitory activity in an in vitro assay using recombinant SIRT1, with high selectivity over SIRT2 and SIRT3. Mechanistic study by means of kinetic analysis, mass spectroscopy, and computation indicated that the enol form of compound **2k** nucleophilically attacks NAD^+ in the active site of SIRTs to afford the stable compound **2k**−ADP−ribose conjugate **5**, leading to inhibition of the enzyme activity. Compound **2k** also caused a dose-dependent increase of p53 acetylation in human colon cancer HCT116 cells, indicating inhibition of SIRT1 in the cells. These results have implications for the development of selective sirtuin inhibitors by means of mechanism-based drug design.

Introduction

Sirtuins catalyze the deacetylation of acetylated lysine residues of proteins using NAD^+ as a cofactor and are involved in a variety of cellular functions, including glucose homeostasis, lifespan extension, cell cycle regulation, apoptosis, DNA repair, and neurodegeneration.[1] Humans have seven distinct sirtuin gene products (SIRT1−7). SIRT1 is localized in the nucleus and modulates gene expression by deacetylating proteins, including histone H4,[2] p53,[3] and BCL6.[4] SIRT2 is localized to the cytoplasm and has been implicated in the process of cell division via deacetylation of α-tubulin.[5] SIRT3 and SIRT4 are mitochondrial proteins that are responsible for activation of mitochondrial functions[6] and insulin secretion,[7] respectively. SIRT5 is also localized in mitochondria, but the function of SIRT5 is not yet well understood.[2] SIRT6, which is localized in the nucleus, has recently been reported to be a deacetylase of lysine 9 of histone H3, playing a role in regulation of telomere metabolism and function.[8] SIRT7 is also localized in the nucleus and is involved in the activation of RNA polymerase I transcription, but its substrates have yet to be identified.[9] Although the functions of SIRTs have not yet been fully understood, as mentioned above, they have been suggested to be associated with various disease states, including cancer and neurodegenerative disorders.[4,10] To date, several classes of SIRT inhibitors have been reported,[11] including 6-chloro-2,3,4,9-tetrahydro-1*H*-carbazole-1-carboxamide (EX-527),[12] 8-bromo-1,2-dihydro-2-phenyl-3*H*-naphtho[2,1-*b*]pyran-3-one (HR73),[13] and 2-cyano-3-[5-(2,5-dichlorophenyl)-2-furanyl]-*N*-5-quinolinyl-2-propenamide (AGK2).[10c] Biological studies using these

(1) (a) Oberdoerffer, P.; Sinclair, D. A. *Nat. Rev. Mol. Cell. Biol.* **2007**, *8*, 692–702. (b) Westphal, C. H.; Dipp, M. A.; Guarente, L. *Trends Biochem. Sci.* **2007**, *32*, 555–560. (c) Yamamoto, H.; Schoonjans, K.; Auwerx, J. *Mol. Endocrinol.* **2007**, *21*, 1745–1755.

(2) Michishita, E.; Park, J. Y.; Burneskis, J. M.; Barrett, J. C.; Horikawa, I. *Mol. Biol. Cell* **2005**, *16*, 4623–4635.

(3) (a) Luo, J.; Nikolaev, A. Y.; Imai, S.; Chen, D.; Su, F.; Shiloh, A.; Guarente, L.; Gu, W. *Cell* **2001**, *107*, 137–148. (b) Vaziri, H.; Dessain, S. K.; Ng Eaton, E.; Imai, S. I.; Frye, R. A.; Pandita, T. K.; Guarente, L.; Weinberg, R. A. *Cell* **2001**, *107*, 149–159. (c) Langley, E.; Pearson, M.; Faretta, M.; Bauer, U. M.; Frye, R. A.; Minucci, S.; Pelicci, P. G.; Kouzarides, T. *EMBO J.* **2002**, *21*, 2383–2396.

(4) Heltweg, B.; Gatbonton, T.; Schuler, A. D.; Posakony, J.; Li, H.; Goehle, S.; Kollipara, R.; Depinho, R. A.; Gu, Y.; Simon, J. A.; Bedalov, A. *Cancer Res.* **2006**, *66*, 4368–4377.

(5) (a) North, B. J.; Marshall, B. L.; Borra, M. T.; Denu, J. M.; Verdin, E. *Mol. Cell* **2003**, *11*, 437–444. (b) Inoue, T.; Hiratsuka, M.; Osaki, M.; Oshimura, M. *Cell Cycle* **2007**, *6*, 1011–1018.

(6) Shi, T.; Wang, F.; Stieren, E.; Tong, Q. *J. Biol. Chem.* **2005**, *280*, 13560–13567.

(7) (a) Argmann, C.; Auwerx, J. *Cell* **2006**, *126*, 837–839. (b) Ahuja, N.; Schwer, B.; Carobbio, S.; Waltregny, D.; North, B. J.; Castronovo, V.; Maechler, P.; Verdin, E. *J. Biol. Chem.* **2007**, *282*, 33583–33592.

(8) Michishita, E.; McCord, R. A.; Berber, E.; Kioi, M.; Padilla-Nash, H.; Damian, M.; Cheung, P.; Kusumoto, R.; Kawahara, T. L.; Barrett, J. C.; Chang, H. Y.; Bohr, V. A.; Ried, T.; Gozani, O.; Chua, K. F. *Nature* **2008**, *452*, 492–496.

(9) Ford, E.; Voit, R.; Liszt, G.; Magin, C.; Grummt, I.; Guarente, L. *Genes Dev.* **2006**, *20*, 1075–1080.

(10) (a) Milne, J. C.; Denu, J. M. *Curr. Opin. Chem. Biol.* **2008**, *12*, 11–17. (b) Itoh, Y.; Suzuki, T.; Miyata, N. *Curr. Pharm. Des.* **2008**, *14*, 529–544. (c) Outeiro, T. F.; Kontopoulos, E.; Altmann, S. M.; Kufareva, I.; Strathearn, K. E.; Amore, A. M.; Volk, C. B.; Maxwell, M. M.; Rochet, J. C.; McLean, P. J.; Young, A. B.; Abagyan, R.; Feany, M. B.; Hyman, B. T.; Kazantsev, A. G. *Science* **2007**, *317*, 516–519. (d) Biel, M.; Wascholowski, V.; Giannis, A. *Angew. Chem., Int. Ed.* **2005**, *44*, 3186–3216.

(11) Neugebauer, R. C.; Sippl, W.; Jung, M. *Curr. Pharm. Des.* **2008**, *14*, 562–573.

(12) (a) Napper, A. D.; Hixon, J.; McDonagh, T.; Keavey, K.; Pons, J. F.; Barker, J.; Yau, W. T.; Amouzegh, P.; Flegg, A.; Hamelin, E.; Thomas, R. J.; Kates, M.; Jones, S.; Navia, M. A.; Saunders, J. O.; DiStefano, P. S.; Curtis, R. *J. Med. Chem.* **2005**, *48*, 8045–8054. (b) Solomon, J. M.; Pasupuleti, R.; Xu, L.; McDonagh, T.; Curtis, R.; DiStefano, P. S.; Huber, L. J. *Mol. Cell. Biol.* **2006**, *26*, 28–38.

 © 2009 American Chemical Society

Scheme 1. Proposed Catalytic Mechanism for the Deacetylation of Acetylated Lysine by Sirtuins

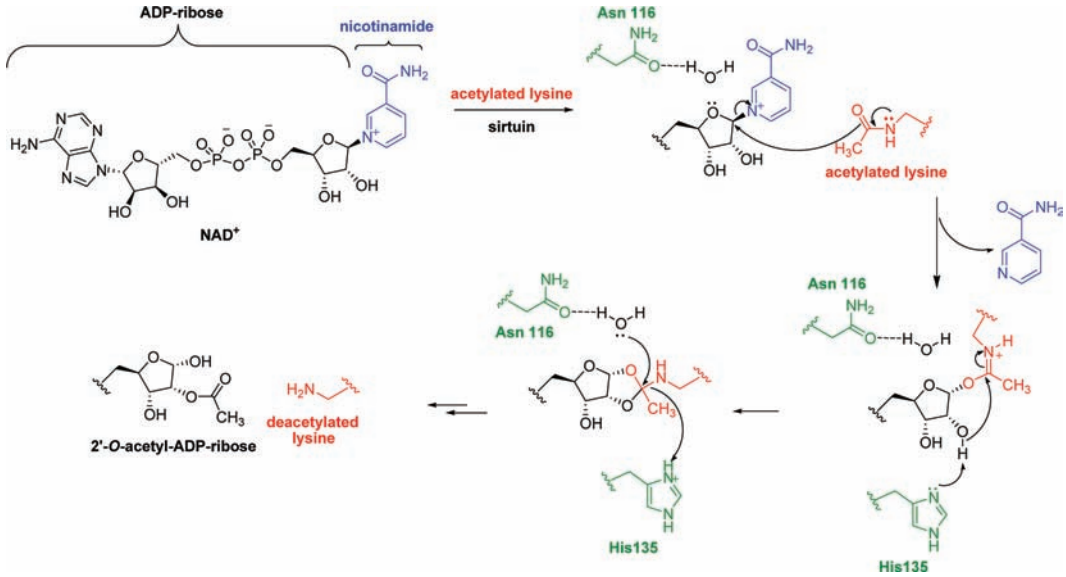

SIRT inhibitors have uncovered the functions of the enzyme and raised the possibility that SIRT inhibitors could be candidate anticancer agents, anti-HIV agents, and antiparkinsonian agents.[4,10c,12,13] Thus, SIRT inhibitors are of interest not only as tools for elucidating in detail the biological functions of the enzyme, but also as potential therapeutic agents.[14]

The deacetylation of proteins catalyzed by sirtuins has been shown to be NAD^+-dependent, releasing nicotinamide and 2′-*O*-acetyl−ADP−ribose.[15] Marmorstein and co-workers reported a high-resolution structural analysis of the ternary complex of yeast Hst2 (homologue of SIRTs) with an acetylated histone H4 peptide and a stable NAD^+ analogue, carba-NAD^+, as well as a ternary complex with ADP−ribose.[16] These crystal structures and a detailed analysis of the catalytic mechanism utilizing various acetylated lysine analogues[17] have led to a solid understanding of the catalytic mechanism of the deacetylation of acetylated lysine substrates by sirtuins (Scheme 1). First, the oxygen of the acetylated lysine substrate attacks the 1′-carbon of the ribose ring of NAD^+ via an S_N2-like mechanism, releasing nicotinamide.[17a,18] Next, the resulting imido ester intermediate is attacked by the 2′-OH group of the ADP ribose activated by His 135 (Hst2 numbering) to form a cyclic intermediate.[17b] Finally, cleavage of the acetal analogue by water coordinated to Asn 116 and protonated His 135 affords deacetylated lysine and 2′-*O*-acetyl−ADP−ribose. This proposed catalytic mechanism for the deacetylation of acetylated lysine substrates provides a basis for the design of selective sirtuin inhibitors. Recently, thioacetyl lysine peptides were identified as mechanism-based sirtuin inhibitors.[19] However, it is difficult to use them for cellular studies due to their poor membrane permeability resulting from their peptide structure; also, thioamide compounds sometimes show toxicity.[20] These considerations led us to design a new type of mechanism-based SIRT inhibitor. Herein, we report the SIRT-inhibitory activity, inhibitory mechanism, and cellular activity of a small-molecular acetylated lysine analogue, which was designed on the basis of the proposed catalytic mechanism of SIRTs.

Results and Discussion

Molecular Design. Our approach takes advantage of the inherent binding affinity of SIRTs for both an acetylated lysine substrate and NAD^+, and also exploits the SIRT-directed synthesis of a bisubstrate analogue from an acetylated lysine substrate and NAD^+, in which the acetylated lysine substrate is linked to ADP−ribose, a partial structure of NAD^+, via a stable carbon−carbon bond.

Jung and co-workers reported that acetylated lysine analogue **1** (Figure 1) is deacetylated by SIRT1, and compound **1** can be used as a substrate for fluorescent SIRT1 enzyme assays.[21] In designing selective SIRT inhibitors, we focused initially on the small-molecular SIRT1 substrate **1**. On the basis of the structure of **1**, we designed acetylated lysine analogues **2** (Figure 1) in

(13) Pagans, S.; Pedal, A.; North, B. J.; Kaehlcke, K.; Marshall, B. L.; Dorr, A.; Hetzer-Egger, C.; Henklein, P.; Frye, R.; McBurney, M. W.; Hruby, H.; Jung, M.; Verdin, E.; Ott, M. *PLoS Biol.* **2005**, *3*, e41.
(14) Lavu, S.; Boss, O.; Elliott, P. J.; Lambert, P. D. *Nat. Rev. Drug Discovery* **2008**, *7*, 841–853.
(15) (a) Imai, S.; Armstrong, C. M.; Kaeberlein, M.; Guarente, L. *Nature* **2000**, *403*, 795–800. (b) Landry, J.; Sutton, A.; Tafrov, S. T.; Heller, R. C.; Stebbins, J.; Pillus, L.; Sternglanz, R. *Proc. Natl. Acad. Sci. U.S.A.* **2000**, *97*, 5807–5811. (c) Sauve, A. A.; Celic, I.; Avalos, J.; Deng, H.; Boeke, J. D.; Schramm, V. L. *Biochemistry* **2001**, *40*, 15456–15463. (d) Chang, J. H.; Kim, H. C.; Hwang, K. Y.; Lee, J. W.; Jackson, S. P.; Bell, S. D.; Cho, Y. *J. Biol. Chem.* **2002**, *277*, 34489–34498. (e) Sauve, A. A.; Schramm, V. L. *Biochemistry* **2003**, *42*, 9249–9256.
(16) Zhao, K.; Harshaw, R.; Chai, X.; Marmorstein, R. *Proc. Natl. Acad. Sci. U.S.A.* **2004**, *101*, 8563–8568.
(17) (a) Smith, B. C.; Denu, J. M. *J. Am. Chem. Soc.* **2007**, *129*, 5802–5803. (b) Smith, B. C.; Denu, J. M. *Biochemistry* **2006**, *45*, 272–282.
(18) Hu, P.; Wang, S.; Zhang, Y. *J. Am. Chem. Soc.* **2008**, *130*, 16721–16728.
(19) (a) Smith, B. C.; Denu, J. M. *Biochemistry* **2007**, *46*, 14478–14486. (b) Fatkins, D. G.; Monnot, A. D.; Zheng, W. *Bioorg. Med. Chem. Lett.* **2006**, *16*, 3651–3656.
(20) (a) Ruse, M. J.; Waring, R. H. *Toxicol. Lett.* **1991**, *58*, 37–41. (b) Zhang, J.; Wang, H.; Yu, H. *Toxicol. Appl. Pharmacol.* **2007**, *224*, 81–88. (c) Kang, J. S.; Wanibuchi, H.; Morimura, K.; Wongpoomchai, R.; Chusiri, Y.; Gonzalez, F. J.; Fukushima, S. *Toxicol. Appl. Pharmacol.* **2008**, *228*, 295–300. (d) Eriksson, C.; Brittebo, E. B. *Toxicol. Lett.* **1995**, *76*, 203–208. (e) Coppola, G. M.; Anjaria, H.; Damon, R. E. *Bioorg. Med. Chem. Lett.* **1996**, *6*, 139–142.
(21) Heltweg, B.; Dequiedt, F.; Marshall, B. L.; Brauch, C.; Yoshida, M.; Nishino, N.; Verdin, E.; Jung, M. *J. Med. Chem.* **2004**, *47*, 5235–5243.
(22) Bitterman, K. J.; Anderson, R. M.; Cohen, H. Y.; Latorre-Esteves, M.; Sinclair, D. A. *J. Biol. Chem.* **2002**, *277*, 45099–45107.

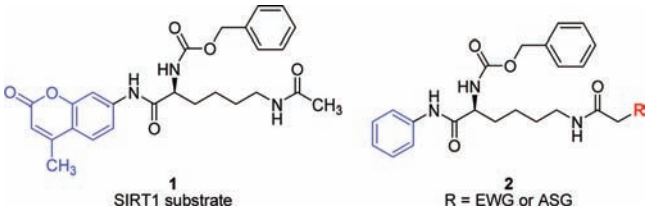

Figure 1. Structures of small-molecular SIRT1 substrate **1** and acetylated lysine analogues **2**.

Scheme 2. Possible Mechanism of Sirtuin Inhibition by in Situ Formation of a Substrate Analogue−ADP−Ribose Conjugate

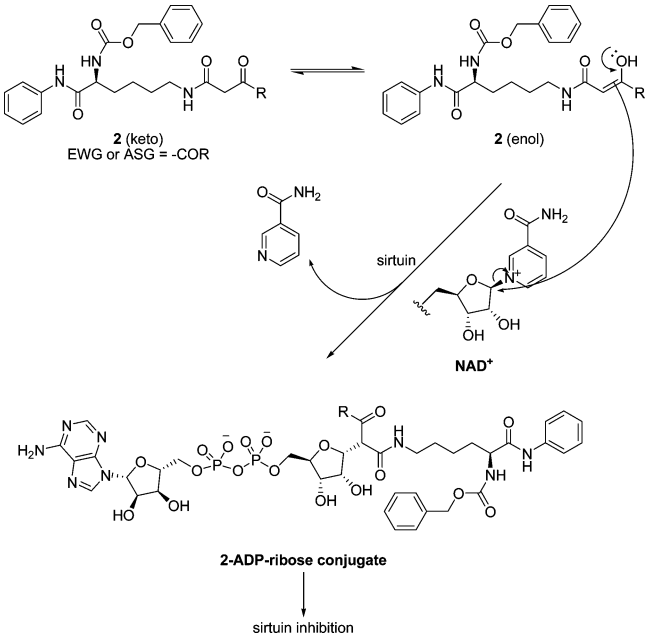

which the coumarin structure is replaced with a simple benzene ring and various electron-withdrawing groups (EWGs) or anion-stabilizing groups (ASGs) are introduced at the α-position of the acetamide. The introduction of EWG or ASG at this position would enhance enol or anion formation of the acetylated lysine analogues, which in turn would increase the nucleophilicity of the α-carbon. If the nucleophilicity of the α-carbon is higher than that of the oxygen of acetamide, nucleophilic attack on NAD^+ should occur at the α-carbon (Scheme 2). The formation of the carbon−carbon bond, which is thermodynamically highly stable, would generate a stable acetylated lysine−ADP−ribose conjugate. We anticipated that this in situ generation of the conjugate might lead to potent SIRT inhibition, because the in situ-generated analogue would occupy both the acetylated lysine-binding pocket and the NAD^+-binding pocket of SIRTs.

Synthesis. The compounds designed and prepared for this study are shown in Table 1. The acetylated lysine analogues **2a**−**z** were synthesized as outlined in Scheme 3. 2-Benzyloxycarbonylamino-6-*tert*-butoxycarbonylaminohexanoic acid **3** was allowed to react with aniline in the presence of EDCI and HOBt to yield the corresponding anilide. Removal of the Boc group of the anilide gave amine **4**. Condensation of amine **4** with an appropriate carboxylic acid in the presence of EDCI and HOBt afforded compounds **2a**−**c**, **2f**−**i**, **2k**, **2o**, and **2x**. Amine **4** underwent reaction with diketene in MeOH to give acetoacetamide **2v**. Compounds **2w** and **2z** were obtained by the reaction between amine **4** and an appropriate carboxylic chloride in the presence of Et_3N and DMAP in CH_2Cl_2. Amine **4** was refluxed

Table 1. SIRT1 Inhibition Data for Compounds **2a**−**z**[a,b,c]

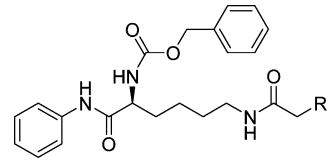

compound	R	inhibition at 300 μM (%)	IC_{50} (μM)
2a	−CN	50 ± 7.9	300 ± 6.2
2b	$-CF_3$	44 ± 17	>300
2c	$-SCH_3$	32 ± 20	>300
2d	$-SOCH_3$	46 ± 3.0	>300
2e	$-SO_2CH_3$	56 ± 1.9	N.D.[d]
2f	2-CF_3Ph	49 ± 13	>300
2g	4-CF_3Ph	41 ± 20	>300
2h	2-NO_2Ph	40 ± 12	>300
2i	4-NO_2Ph	51 ± 17	N.D.[d]
2j	$-COOCH_3$	92 ± 1.2	35 ± 5.2
2k	−COOEt	91 ± 1.3	3.9 ± 0.29
2l	−COO*n*-Pr	73 ± 0.72	62 ± 3.7
2m	−COO*i*-Pr	72 ± 5.1	47 ± 5.3
2n	−COO*n*-Bu	64 ± 6.1	73 ± 3.2
2o	−COO*t*-Bu	6.0 ± 0.64	>300
2p	$-COOCH_2$-*c*-Pr	93 ± 1.2	14 ± 2.6
2q	$-COOCH_2CF_3$	94 ± 1.5	15 ± 3.1
2r	$-COOCH_2Ph$	71 ± 4.3	96 ± 4.8
2s	$-CONH_2$	25 ± 2.3	>300
2t	$-CONHCH_3$	24 ± 2.5	>300
2u	$-CON(CH_3)_2$	20 ± 1.3	>300
2v	$-COCH_3$	45 ± 6.0	>300
2w	−COEt	67 ± 1.2	88 ± 3.9
2x	−CO*n*-Pr	78 ± 5.2	56 ± 5.3
2y	$-COCF_3$	7.9 ± 0.92	>300
2z	−COPh	37 ± 7.4	>300

[a] SIRT1 was preincubated with NAD^+ and compounds **2a**−**z**, and then acetylated lysine substrate was added. [b] Values are means ± SD determined from at least three experiments. [c] Nicotinamide[22] (IC_{50} = 25 ± 5.1 μM) and EX-527[12] (IC_{50} = 1.4 ± 0.23 μM) were used as positive controls. [d] N.D. = not determined.

with ethyl 4,4,4-trifluoroacetoacetate in toluene to give trifluoroacetoacetamide **2y**. Oxidation of sulfide **2c** with 1 and 2 equiv of MCPBA in CH_2Cl_2 gave sulfoxide **2d** and sulfone **2e**, respectively. Treatment of ethyl ester **2k** with ammonia in MeOH resulted in ester exchange to afford methyl ester **2j**, whereas treatment of **2k** with methylamine or dimethylamine yielded methylamide **2t** and dimethylamide **2u**, respectively. Esters **2l**−**n** and **2p**−**r** were obtained from *tert*-butyl ester **2o** by removal of the *tert*-butyl group of **2o**, and condensation of the carboxylic acid with an appropriate alcohol in the presence of EDCI and DMAP. Similarly, amide **2s** was obtained by removal of the *tert*-butyl group of **2o**, and condensation between the carboxylic acid and ammonia in the presence of EDCI and HOBt.

Enzyme Assay. To evaluate the potency of acetylated lysine analogues **2a**−**z**, an in vitro assay using recombinant SIRT1 was initially performed. SIRT1 was incubated with NAD^+ and compounds **2a**−**z** before the addition of acetylated lysine substrate, in anticipation of in situ generation of the substrate analogue−ADP−ribose conjugate. The results are summarized in Table 1. Compounds **2a**−**i**, which do not have a keto moiety as an EWG, showed SIRT1-inhibitory activity, although the potencies were low (32−56% inhibition at a concentration of 300 μM). Ester compounds **2j**−**r** exhibited greater potencies than did compounds **2a**−**i**, with the exception of **2o** (R = COO*t*-Bu), which was less potent. In the ester series, the strongest inhibition was observed with ethyl ester **2k**, which dose-

Scheme 3. Synthesis of Acetylated Lysine Analogues **2a**−**z**[a]

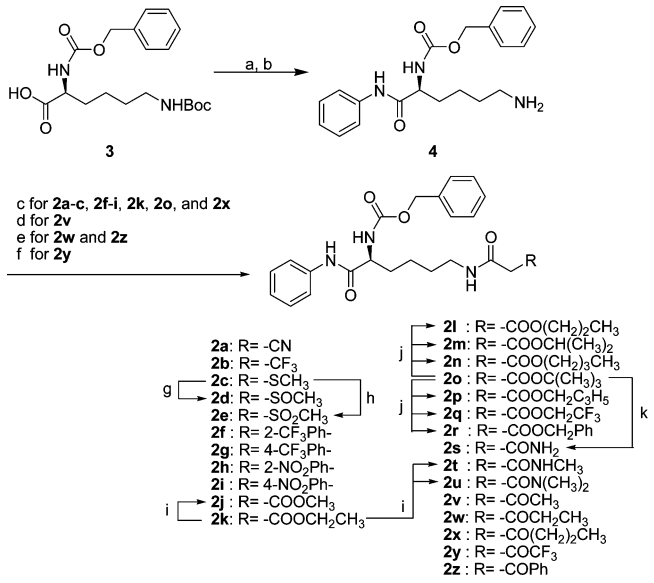

[a] (a) Aniline, 1-ethyl-3-(3-dimethylaminopropyl)carbodiimide (EDCI), 1-hydroxybenzotriazole hydrate (HOBt·H_2O), DMF, room temperature, 94%; (b) HCl, AcOEt, room temperature, 99%; (c) RCH_2COOH, EDCI, HOBt·H_2O, Et_3N, DMF, room temperature, 33−89%; (d) diketene, Et_3N, MeOH, room temperature, 93%; (e) $RCOCH_2COCl$, DMAP, Et_3N, CH_2Cl_2, room temperature, 68−72%; (f) ethyl 4,4,4-trifluoroacetate, toluene, reflux, 74%; (g) MCPBA (1 equiv), CH_2Cl_2, room temperature, 84%; (h) MCPBA (2 equiv), CH_2Cl_2, room temperature, 86%; (i) R_2NH, MeOH, room temperature, 37−62%; (j) (i) TFA, CH_2Cl_2, room temperature, 78%; (ii) ROH, EDCI, DMAP, THF or DMF, room temperature, 20−81%; (k) (i) TFA, CH_2Cl_2, room temperature, 78%; (ii) NH_3, EDCI, HOBt·H_2O, THF, room temperature, 45%.

dependently inhibited SIRT1 activity with an IC_{50} of 3.9 μM. Methyl ester **2j**, which has a smaller alkyl group than **2k**, was found to be an about 9-fold less potent inhibitor than ethyl ester **2k**. Conversion of the ethyl group of **2k** to larger alkyl groups (**2l**−**r**) also decreased the potency, although cyclopropylmethyl **2p** and trifluoroethyl **2q**, in which the size of the alkyl group is quite similar to that of **2k**, retained potency to some extent. These data indicate the importance of the alkyl group size for SIRT1-inhibitory activity. To investigate further the structural requirements for the inhibition of SIRT1, carboxamides **2s**−**u** and ketones **2v**−**z** were also tested. Basically, compounds **2s**−**z** showed weaker activity than the ester series. In particular, methyl carboxamide **2t** and ethyl ketone **2w** were less potent than the corresponding ester **2j**, and *n*-propyl ketone **2x** was less potent than the corresponding ester **2k**. These results suggest that the alkoxy moiety of the ester inhibitors is crucial for potent inhibition of SIRT1.

To examine the isoform selectivity of compound **2k**, the most potent compound in this study, we next conducted enzyme assays using recombinant SIRT1, SIRT2, and SIRT3. Compound **2k** showed 17-fold and more than 77-fold selectivity for SIRT1 over SIRT 2 and SIRT3, respectively (IC_{50} for SIRT2 = 65 μM; IC_{50} for SIRT3 > 300 μM).

Analysis of the Inhibitory Mechanism. To investigate the mechanism of SIRT1 inhibition by compound **2k**, we initially performed an enzyme kinetic assay using various concentrations of compound **2k**. The data were plotted as 1/rate (V) versus 1/[acetylated lysine substrate] (Lineweaver−Burk plot) at each concentration of compound **2k** (Figure 2). Because the lines

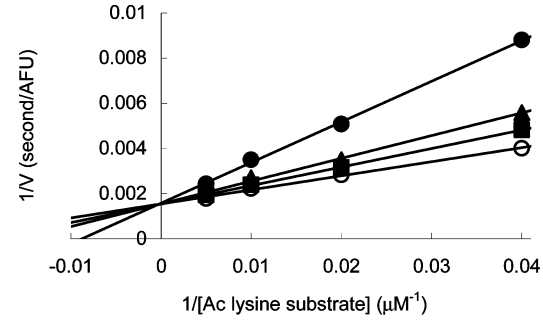

Figure 2. Reciprocal rate versus reciprocal acetylated lysine substrate in the presence of 30 (●), 10 (▲), 3 (■), and 0 (○) μM **2k**.

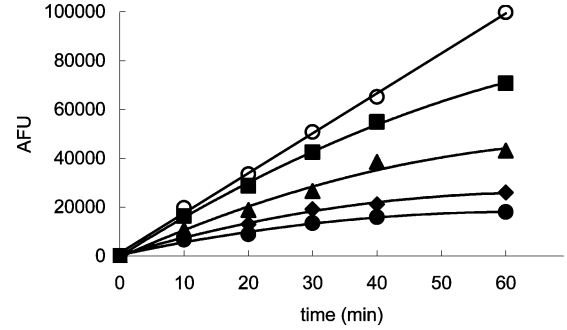

Figure 3. Plots of product formation versus time in the absence (○) and presence of 10 (■), 30 (▲), 100 (◆), and 300 (●) μM **2k**.

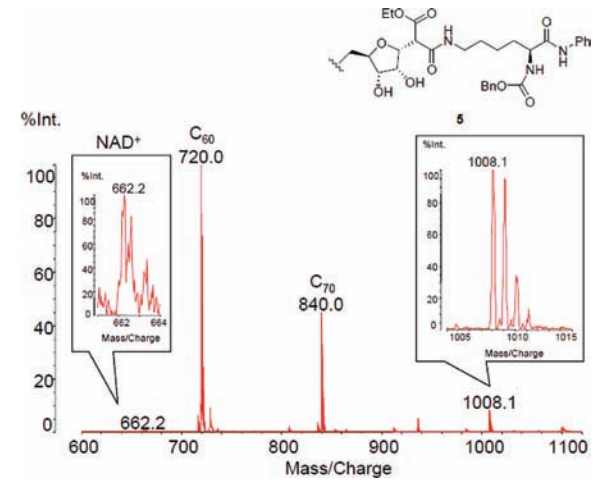

Figure 4. Mass spectrometric detection of compound **2k**−ADP−ribose conjugate **5**. C_{60} (*m*/*z* 720.0) and C_{70} (*m*/*z* 840.0) were used as internal standards.

intersected at the 1/V axis, compound **2k** is a competitive inhibitor with respect to the acetylated lysine substrate, with K_i = 9.5 μM.

We also carried out an SIRT1 inhibition assay by simultaneous incubation of SIRT1 with NAD^+, compound **2k**, and acetylated lysine substrate. The IC_{50} value of **2k** in the simultaneous incubation study was 20 μM (K_i = 67 μM) (Figure S1), which is higher than that in the preincubation study. Next, we performed another SIRT1 inhibition assay in which compound **2k** and NAD^+ were incubated in the absence of both SIRT1 and acetylated lysine substrate, followed by the addition of these two components. The IC_{50} value of **2k** in the control experiment was 23 μM (K_i = 70 μM) (Figure S2), which is also higher than that in the **2k**, NAD^+, and SIRT1 preincubation

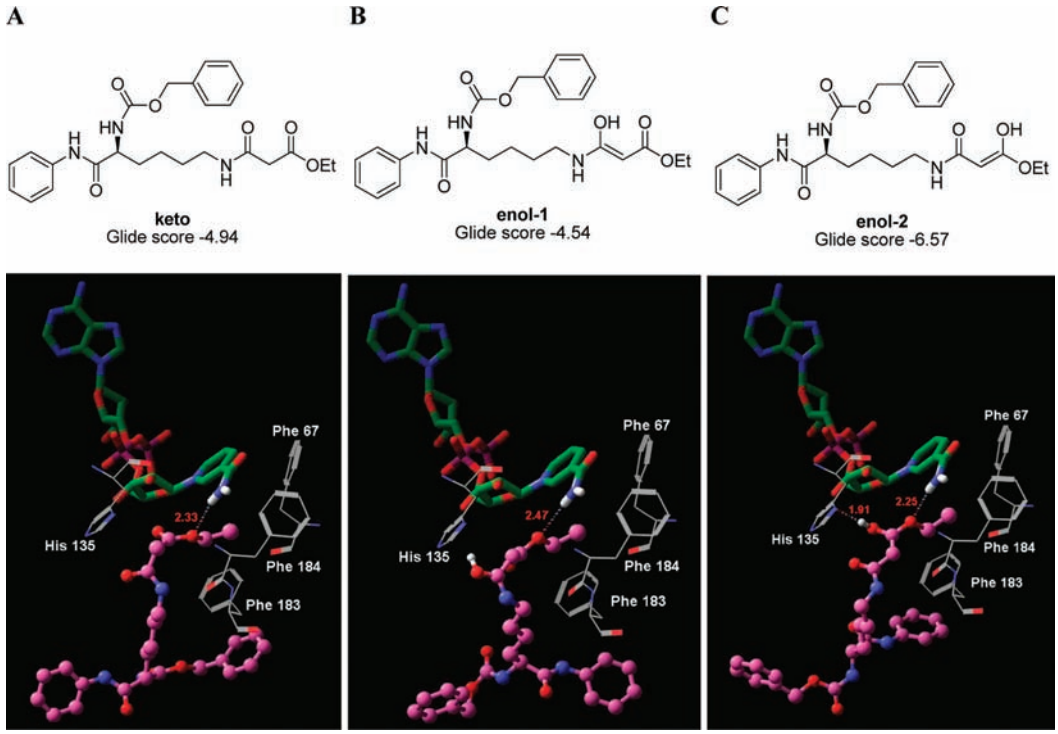

Figure 5. View of the lowest-energy conformation of the keto (A), enol-1 (B), and enol-2 (C) forms of **2k** (ball and stick) docked into the yeast Hst2 (homologue of SIRTs) catalytic core. Amino acid residues lying next to the ethoxycarbonyl group of **2k** and NAD^+ are displayed in the wire and tube graphic, respectively. Glide scores are expressed in kcal/mol.

study. In addition, the IC_{50} values of compound **2p**, the second most potent inhibitor in this study, in the simultaneous incubation study, and in the **2p** and NAD^+ preincubation study, were determined to be 72 and 74 μM, respectively, which are also higher than the IC_{50} value (14 μM) in the **2p**, NAD^+, and SIRT1 preincubation study. These two control experimental results indicate that compounds **2k** and **2p** react with NAD^+ in the active site of SIRT1 to cause the inhibition.

To determine whether inhibition by **2k** is time-dependent, the time course of product formation was monitored in the absence and presence of compound **2k** (Figure 3). These experiments were performed by simultaneous incubation of SIRT1 with NAD^+, compound **2k**, and acetylated lysine substrate. The inhibition was time-dependent, showing nonlinear progress curves and reaching a plateau value. We performed a similar study using compound **2p**, and the results were similar to those obtained with compound **2k** (Figure S3).

To gain further insight into the mechanism of SIRT1 inhibition by compound **2k**, a mass spectroscopic analysis of a mixture of SIRT1 incubated with NAD^+ and compound **2k** was performed. If compound **2k** reacts with NAD^+ at the α-position of the acetamide as expected, compound **2k**−ADP−ribose conjugate **5** (Figure 4) should be generated. As depicted in Figure 4, while the peak of NAD^+ was observed at *m*/*z* 662.2, a significant peak at *m*/*z* 1008.1 was also observed. This peak corresponds to the predicted molecular weight of compound **2k**−ADP−ribose conjugate **5**. The peak was dependent on the presence of SIRT1 and compound **2k**; that is, it was not detected in the absence of SIRT1 or compound **2k** (Figure S4). These results indicate that compound **5** was generated as a result of SIRT1-guided reaction of compound **2k** and NAD^+. In addition, a similar mass spectroscopic analysis using compound **2p** gave a different mass for the adduct (*m*/*z* 1033.4) (Figure S5), again indicating formation of the conjugate with ADP−ribose. The data from the mass spectroscopic analysis supported the idea that compound **2** nucleophilically attacks NAD^+ in the active site of SIRT1, affording compound **2**−ADP−ribose conjugate, which causes SIRT1 inhibition. Because the amount of the conjugate cannot be measured in a quantitative manner with mass spectroscopic analysis, it cannot be established whether this is the major inhibition pathway. Nevertheless, the mass spectroscopic evidence in addition to the enzyme assay results of preincubation versus coincubation and the observation of time-dependent inhibition are consistent with the hypothesis that the proposed mechanism (Scheme 2) is the main pathway for SIRT1 inhibition.

To examine the inhibition mechanism in more detail, we attempted to measure the population of the enol form of compound **2k** in the presence of SIRT1 using ^1H NMR, but found that the NMR spectra were too complicated to interpret. We then calculated the lowest energy conformations of the keto form and two enol forms (enol-1 and enol-2) of **2k** docked into a model based on the crystal structure of yeast Hst2 (PDB code 1Q1A),[16] a homologue of SIRTs, using the software package Glide 3.5[23] (Figure 5). The docking scores (Glide scores) of the keto, enol-1, and enol-2 form of **2k** were −4.94, −4.54, and −6.57, respectively, indicating that enol-2 is the most stable tautomer of the three in the active site of SIRTs. An inspection of the Hst2/**2k** complex suggests that the ethyl group of **2k** is located in the hydrophobic pocket formed by Phe 67, Phe 183,

(23) (a) Friesner, R. A.; Banks, J. L.; Murphy, R. B.; Halgren, T. A.; Klicic, J. J.; Mainz, D. T.; Repasky, M. P.; Knoll, E. H.; Shelley, M.; Perry, J. K.; Shaw, D. E.; Francis, P.; Shenkin, P. S. *J. Med. Chem.* **2004**, *47*, 1739–1749. (b) Halgren, T. A.; Murphy, R. B.; Friesner, R. A.; Beard, H. S.; Frye, L. L.; Pollard, W. T.; Banks, J. L. *J. Med. Chem.* **2004**, *47*, 1750–1759.
(24) Guthrie, J. P.; O'Leary, S. *Can. J. Chem.* **1975**, *53*, 2150–2156.
(25) Belova, N. V.; Oberhammer, H.; Shlykov, S. A. *J. Phys. Chem. A* **2008**, *112*, 4355–4359.

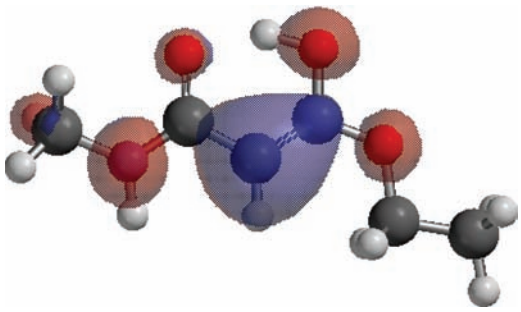

Figure 6. HOMO calculation of (*E*)-3-ethoxy-3-hydroxy-*N*-methylacrylamide.

and Phe 184, and the oxygen of the ethoxy group of **2k** forms a hydrogen bond with the carboxamide group of NAD^+ (the distance between the hydrogen of the carboxamide of NAD^+ and the oxygen of the ethoxy group of **2k** is 2.25−2.47 Å). In addition, in the complex of Hst2 with the enol-2 form of **2k**, a hydrogen bond can exist between the enol and the imidazole group of His 135 (the distance between the hydrogen of the enol and the nitrogen of the imidazole is 1.91 Å). These calculation results suggest that the enol-2 form is favored in the active site of SIRTs due to the interaction with the imidazole of His.[24] The results of similar calculations for nitrile **2a**, methyl ester **2j**, methyl ketone **2v**, and *n*-propyl ketone **2x** are summarized in Table S1. Consistent with the results of the enzyme inhibition assays, the Glide scores of these compounds were worse than that of **2k**, which can be explained by the lack of a hydrogen bond between the ethoxy group of **2k** and the carboxamide group of NAD^+ (in the cases of **2v** and **2x**), and/or the lack of hydrophobic interaction between the ethyl group of **2k** and three phenylalanines (in the cases of **2a**, **2j**, and **2v**). Regarding the relative energies of the keto and enol tautomers before binding, the tautomeric properties of malonamic acid methyl ester, $NH_2C(O)-CH_2-C(O)OCH_3$, have recently been investigated by means of gas-phase electron diffraction and quantum chemical calculations.[25] The calculations showed that the keto form possesses much lower energy than do the two enol forms. This report suggests that compound **2k** would exist in the keto form before binding, and our calculations indicate that enol-2 is the most stable tautomer in the active site of SIRTs. Taken together, these results are consistent with the idea that the keto form of **2k** is recognized by sirtuins and taken into the active site, where it is tautomerized to the more stable enol-2 form.

We next calculated the highest occupied molecular orbital (HOMO) of (*E*)-3-ethoxy-3-hydroxy-*N*-methylacrylamide, a partial structure of the enol-2 form of compound **2k**. As shown in Figure 6, while lower values of HOMO were seen over the oxygen of the acetamide, higher values of HOMO were confined to the α-carbon of the acetamide, indicating that the α-carbon of the acetamide is more likely to be involved in nucleophilic attack on NAD^+ than is the oxygen of the acetamide. This calculation is consistent with the observation of compound **2k**−ADP−ribose conjugate **5** in the mass spectroscopic analysis. In addition, this calculation result can explain the selective C-alkylation or acylation in preference to O-alkylation or acylation of malonamic acid derivatives reported so far.[26] Because the results obtained in this calculation study are roughly consistent with the experimental results, these calculations may be helpful in the design of superior sirtuin inhibitors.

Our calculation study has suggested that the imidazole group of histidine residue could promote enol formation of **2k** in the active site of sirtuins. However, the calculation study of malonamic acid methyl ester[25] mentioned above suggested that the tautomerization from keto to enol of **2k** needs high energy. This prompted us to examine whether the enol form of **2k** is formed in the presence of imidazole in various solvents, using ^1H NMR. However, if the enol form was generated, its population was too low to detect. We next examined whether deuterium exchange of **2k** occurs in D_2O/DMSO-d_6 (1/4) medium in the absence and presence of imidazole. No deuterium

Scheme 4. Proposed Mechanism of Inhibition of SIRTs by Compound **2k**

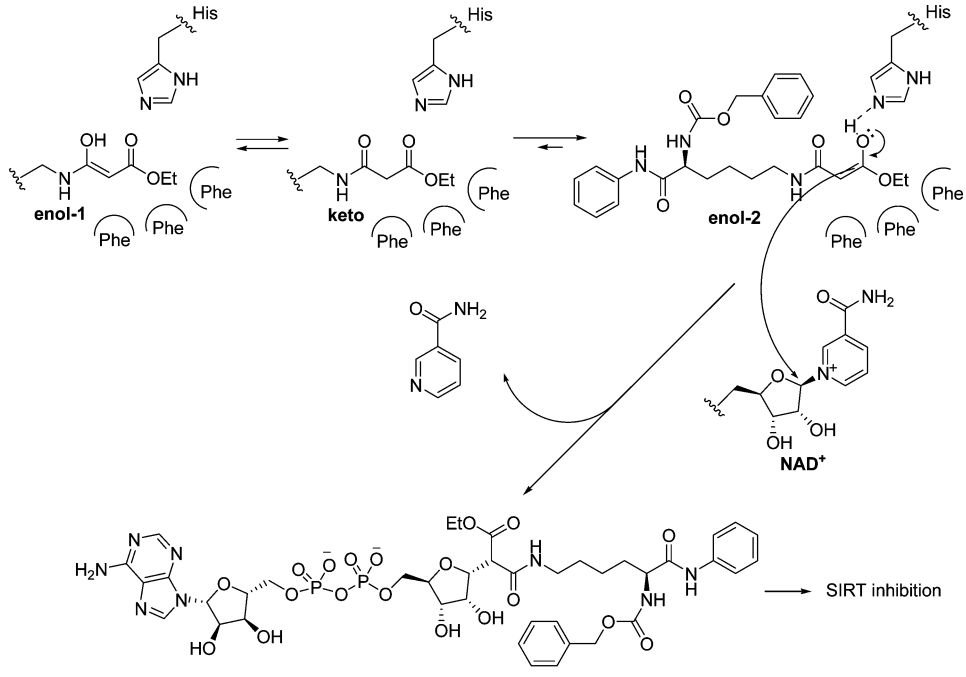

5

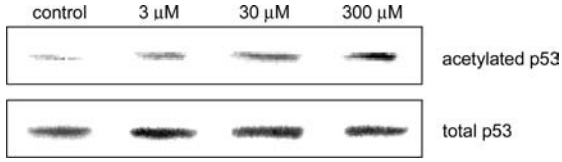

Figure 7. Western blot detection of acetylated p53 levels in HCT116 cells after an 8 h incubation with 20 μM etoposide and 3, 30, and 30 μM compound **2k**.

exchange of **2k** was observed in the absence of imidazole, whereas almost complete deuterium incorporation was observed at the methylene position between the two carbonyl groups of **2k** in the presence of imidazole (Figure S6). These observations clearly indicate that imidazole does enhance the enol formation of **2k**.

On the basis of these results, we propose that compound **2k** is recognized as a substrate by SIRTs and enters the active site, where the enol form of compound **2k**, formation of which is promoted by the imidazole group of His, nucleophilically attacks NAD^+ to afford the stable **2k**−ADP−ribose conjugate **5**, leading to the inhibition of SIRTs (Scheme 4).

Cellular Assay. Unlike thioacetyl peptides, recently reported mechanism-based inhibitors,[19] compound **2k** is a small-molecular SIRT inactivator, which might be active in cellular assays. To test whether this is the case, we performed a cellular assay using Western blot analysis. Because SIRT1 is known to catalyze the deacetylation of p53 in cells with DNA damage,[3] the acetylation level of p53 in human colon cancer HCT116 cells after etoposide-induced DNA damage was analyzed. As can be seen in Figure 7, the level of acetylated p53 was dose-dependently elevated. These results suggest that compound **2k** inactivates SIRT1 in cells and can be used as a tool for probing the biological role of SIRT1.

Conclusion

On the basis of the proposed catalytic mechanism for the deacetylation of acetylated lysine substrates by sirtuins, we designed several small-molecular acetylated analogues as candidate mechanism-based sirtuin inhibitors. Among the synthesized compounds, **2k** showed the most potent SIRT1-inhibitory activity. Kinetic analysis, mass spectroscopic analysis, and computational study suggested that the inhibitory mechanism involves SIRT1-directed synthesis of compound **2k**−ADP−ribose conjugate **5** from acetylated lysine analogue **2k** and NAD^+. Compound **2k** was confirmed to inhibit SIRT1 in a cellular study.

Thus, we have identified a novel lead structure, compound **2k**, from which it should be possible to develop potent and isoform-selective sirtuin inhibitors by modifying the anilino and benzyloxycarbonyl groups. This should be helpful in the development of therapeutic agents for various diseases, as well as tools for studying the biological roles of sirtuins.

Experimental Section

Synthesis of 5-Benzyloxycarbonylamino-5-phenylcarbamoylpentylammonium Chloride (4·HCl). A mixture of *Z*-Lys(Boc)−OH (**3**) (4.46 g, 11.7 mmol), aniline (2.15 g, 23.0 mmol), EDCI (3.36 g, 17.5 mmol), and HOBt·H_2O (2.68 g, 17.5 mmol) in DMF (100 mL) was stirred for 24 h at room temperature. The reaction mixture was poured into water, and the whole was extracted with AcOEt. The AcOEt layer was separated, washed with saturated aqueous $NaHCO_3$ and brine, and was dried over Na_2SO_4. Filtration and concentration in vacuo gave a colorless solid. The solid was suspended in *n*-hexane and collected by filtration to give 5.03 g (94%) of (5-*tert*-butoxycarbonylamino-1-phenylcarbamoylpentyl-)carbamic acid benzyl ester as a colorless solid: ^{1}H NMR (DMSO-d_6, 500 MHz, δ; ppm) 10.00 (1H, s), 7.59 (2H, d, J = 8.2 Hz), 7.53 (1H, d, J = 7.6 Hz), 7.37−7.28 (7H, m), 7.04 (1H, t, J = 7.5 Hz), 6.77 (1H, m), 5.03 (2H, s), 4.11 (1H, m), 2.88 (2H, m), 1.61 (2H, m), 1.35 (2H, s), 1.41−1.22 (4H, m).

To a solution of (5-*tert*-butoxycarbonylamino-1-phenylcarbamoylpentyl)carbamic acid benzyl ester (5.03 g, 11.0 mmol) obtained above in AcOEt (100 mL) was added 4 N HCl/AcOEt (55 mL, 220 mmol) with cooling by an ice-bath. The mixture was stirred for 16 h at room temperature. The resulting solid was collected by filtration and washed with AcOEt to give 3.95 g of **4·HCl** as a colorless solid. The filtrare was evaporated in vacuo. The residue was suspended in ether and collected by filtration to give 0.323 g (total 4.28 g, 99%) of **4·HCl** as a colorless solid: ^{1}H NMR (DMSO-d_6, 500 MHz, δ; ppm) 10.12 (1H, s), 7.80 (2H, broad s), 7.62 (2H, d, J = 7.6 Hz), 7.58 (1H, d, J = 7.9 Hz), 7.37−7.29 (7H, m), 7.05 (1H, t, J = 7.3 Hz), 5.03 (2H, s), 4.17−4.12 (1H, m), 2.76 (2H, broad s), 1.71−1.61 (2H,m), 1.63 (2H, m), 1.47−1.33 (2H, m).

Synthesis of *N*-(5-Benzyloxycarbonylamino-5-phenylcarbamoylpentyl)malonamic Acid Ethyl Ester (2k). To a solution of **4·HCl** (489 mg, 1.25 mmol) obtained above and malonic acid monoethyl ester potassium salt (431 mg, 1.25 mmol) in DMF (20 mL) were added EDCI (362 mg, 1.89 mmol), HOBt (287 mg, 1.87 mmol), and triethylamine (506 mg, 5.00 mmol). The mixture was stirred for 23 h at room temperature. The reaction mixture was poured into water and extracted with AcOEt. The organic layer was separated, washed with brine, and dried over Na_2SO_4. Filtration, concentration in vacuo, and purification by silica gel flash column chromatography (AcOEt/*n*-hexane = 3/1) gave 564 mg (96%) of **2k** as a crude solid, which was recrystallized from AcOEt to give 379 mg of **2k** as colorless crystals: mp 132−135 °C; ^{1}H NMR (DMSO-d_6, 500 MHz, δ; ppm) 10.01 (1H, s), 8.05 (1H, t, J = 5.6 Hz), 7.59 (2H, d, J = 7.9 Hz), 7.54 (1H, d, J = 7.6 Hz), 7.37−7.29 (7H, m), 7.05 (1H, t, J = 7.3 Hz), 5.03 (2H, s), 4.12 (1H,m), 4.05 (3H, q, J = 7.2 Hz), 3.17 (2H, s), 3.04 (2H, m), 1.60 (2H, m), 1.41−1.31 (4H, m), 1.16 (3H, t, J = 7.0 Hz); ^{13}C NMR (DMSO-d_6, 500 MHz, δ; ppm) 171.00, 167.83, 164.87, 156.00, 138.83, 136.90, 128.59, 128.25, 127.70, 127.61, 123.19, 119.15, 65.34, 60.28, 55.28, 42.40, 38.44, 31.37, 28.51, 22.88, 13.89; MS (FAB) m/z 470 (M^+). Anal. Calcd for $C_{25}H_{31}N_3O_5$: C, 63.95; H, 6.65; N, 8.95. Found: C, 63.69; H, 6.65; N, 9.14.

SIRT Enzyme Assays. The SIRT activity assay was performed using SIRT fluorimetric drug discovery kits (AK-555, AK-556, and AK-557, BIOMOL Research Laboratories), according to the supplier's protocol. SIRT (human, recombinant) (15 μL/well), NAD^+ (25 μM), and various concentrations of samples were incubated at 37 °C for 60 min, and Fluor de Lys-SIRT substrate (25 μM) was added to the mixture. Reactions were stopped after 60 min by adding Fluor de Lys Developer II with nicotinamide, which stops further deacetylation. Next, 45 min after addition of this developer, the fluorescence of the wells was measured on a fluorometric reader with excitation set at 360 nm and emission detection set at 460 nm. The value of % inhibition was calculated from the fluorescence readings of inhibited wells relative to those of control wells. The compound concentration resulting in 50% inhibition was determined by plotting log[Inh] versus the logit function of % inhibition. IC_{50} values were determined by means of regression analysis of the concentration/inhibition data.

Lineweaver−Burk Double-Reciprocal Plot Analysis. The assay of SIRT activity was performed using a SIRT1 fluorimetric drug discovery kit (AK-555, BIOMOL Research Laboratories). Fluor de Lys-SIRT substrate (final concentration: 25, 50, 100, or 200 μM) was added to a mixture of SIRT1 (human, recombinant) (15 μL/well), 50 μM NAD^+, and compound **2k** (3, 10, or 30 μM), and the mixture was incubated at 37 °C. Reactions were stopped after 30 min by adding Fluor de Lys Developer II with nicotinamide, which stops further deacetylation. Next, 45 min after addition of

this developer, the fluorescence of the wells was measured on a fluorometric reader with excitation set at 360 nm and emission detection set at 460 nm.

MALDI-TOF/MS Analysis. Reactions were conducted in 20 μL volumes containing 1 mM DTT, 600 μM compound **2k** or **2p**, 500 μM NAD^+, 4 μM SIRT1 (human recombinant) (BIOMOL Research Laboratories), and 20 μM pyridine buffer adjusted to pH 7 with formic acid for 60 s at 25 °C. Controls were run without the compound or the enzyme. The reaction mixtures were subjected to mass spectral analysis utilizing an AXIMA CFR-Plus matrix-assisted laser desorption ionization time-of-flight (MALDI-TOF) instrument (SHIMADZU/KRATOS) in linear negative mode with 20 kV acceleration. α-Cyano-4-hydroxycinnamic acid was used as the matrix, and C_{60} and C_{70} were used as internal standards.

Molecular Modeling. The X-ray structure of yeast Hst2 (PDB code 1Q1A) was used as the target structure for docking. Protein preparation, receptor grid generation, and ligand docking were performed using the software Glide 3.5.[23] Compounds **2k**, **2a**, **2j**, **2v**, and **2x** were docked into the histone H4 binding site of Hst2. The standard precision mode of Glide was used to determine favorable binding poses, which allowed the ligand conformation to be flexibly explored while holding the protein as a rigid structure during docking.

The lower energy conformer of (*E*)-3-ethoxy-3-hydroxy-*N*-methylacrylamide, the partial structure of the enol form of compound **2k**, was searched by a molecular mechanics force field (MMFF)[27] analysis, and HOMO calculation was done with the density functional theories model[28] at the B3LYP/6-311+G** level. The HOMO calculation and graphical representation were performed by using the SPARTAN 06 for Windows software package.

Western Blot Analysis. HCT116 human colon cancer cells were purchased from American type Culture Collection (ATCC, Manassas, VA) and cultured in McCoy5A culture medium containing penicillin and streptomycin, which was supplemented with fetal bovine serum as described in the ATCC instructions. HCT-116 cells (5×10^5) were treated for 8 h with 20 μM etoposide and compound **2k** at the indicated concentrations in 10% FBS-supplemented McCoy's 5A medium, and then collected and extracted with SDS buffer. Protein concentrations of the lysates were determined using a Bradford protein assay kit (Bio-Rad Laboratories); equivalent amounts of proteins from each lysate were resolved in 15% SDS−polyacrylamide gel and then transferred onto nitrocellulose membranes (Bio-Rad Laboratories). After having been blocked for 30 min with Tris-buffered saline (TBS) containing 3% skim milk, the transblotted membrane was incubated overnight at 4 °C with acetylated p53 antibody (Cell Signaling) (1:1000 dilution) or p53 antibody (Calbiochem) (1:1000 dilution) in TBS containing 3% skim milk. The membrane was probed with the primary antibody, and then washed twice with water, incubated with goat antimouse IgG−horseradish peroxidase conjugates (diluted 1:2500) for 2 h at room temperature, and again washed twice with water. The immunoblots were visualized by enhanced chemiluminescence.

Acknowledgment. This work was supported in part by a Grant-in-Aid for Scientific Research from Japan Society for the Promotion of Science, a Grant-in-Aid for Research in Nagoya City University, and a grant from Ichihara International Scholarship Foundation.

Supporting Information Available: Experimental details for the synthesis of compounds **2a**−**z**, Figures S1−6, and Table S1. This material is available free of charge via the Internet at http://pubs.acs.org.

JA807083Y

(26) (a) Williams, D. R.; Benbow, J. W. *J. Org. Chem.* **1988**, *53*, 4643–4644. (b) Venuti, M. C.; Alvarez, R.; Bruno, J. J.; Strosberg, A. M.; Gu, L.; Chiang, H. S.; Massey, I. J.; Chu, N.; Fried, J. H. *J. Med. Chem.* **1988**, *31*, 2145–2152. (c) Poli, G.; Giambastiani, G. *J. Org. Chem.* **2002**, *67*, 9456–9457. (d) Hoffman, R. V.; Madan, S. *J. Org. Chem.* **2003**, *68*, 4876–4885. (e) Scansetti, M.; Hu, X.; McDermott, B. P.; Lam, H. W. *Org. Lett.* **2007**, *9*, 2159–2162.
(27) Halgren, T. A. *J. Comput. Chem.* **1996**, *17*, 490–519.
(28) Kohn, W.; Becks, A. D.; Parr, R. G. *J. Phys. Chem.* **1996**, *100*, 12974–12980.